

Flexoelectric Rectification of Charge Transport in Strain-Graded Dielectrics

Daesu Lee,^{†,‡} Sang Mo Yang,^{†,‡} Jong-Gul Yoon,[§] and Tae Won Noh^{*,†,‡}

[†]IBS-Center for Functional Interfaces of Correlated Electron Systems, Seoul National University, Seoul 151-747, Korea

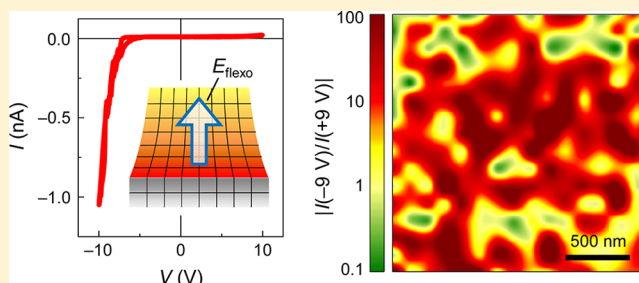
[‡]Department of Physics and Astronomy, Seoul National University, Seoul 151-747, Korea

[§]Department of Physics, University of Suwon, Suwon, Gyeonggi-do 445-743, Korea

S Supporting Information

ABSTRACT: Flexoelectricity is emerging as a fascinating means for exploring the physical properties of nanoscale materials. Here, we demonstrated the unusual coupling between electronic transport and the mechanical strain gradient in a dielectric epitaxial thin film. Utilizing the nanoscale strain gradient, we showed the unique functionality of flexoelectricity to generate a rectifying diode effect. Furthermore, using conductive atomic force microscopy, we found that the flexoelectric effect can govern the local transport characteristics, including spatial conduction inhomogeneities, in thin-film epitaxy systems. Consideration of the flexoelectric effect will improve understanding of the charge conduction mechanism at the nanoscale and may facilitate the advancement of novel nanoelectronic device design.

KEYWORDS: Epitaxial thin film, flexoelectricity, local transport, nanoscale strain gradient



Strain engineering has long served as a foundation for novel material design and improved functionality^{1–3} and has generally assumed the homogeneous strain condition. Recently, however, inhomogeneous strain (i.e., strain gradient) has gained much attention,^{4–7} due to its important role in nanoscale materials via flexoelectricity. Flexoelectricity describes the generation of an internal electric field (or polarization) by the strain gradient.^{8–13} The strain gradient naturally breaks the inversion symmetry and thus can induce an electric response and intriguing phenomena in all dielectrics. Despite this universal nature, the resulting flexoelectric field is quite small ($\leq 10 \text{ V m}^{-1}$) at the macroscopic level. However, for a nanoscale material, in which strain variation can occur over a very short length scale, the flexoelectric field can become large enough ($\geq 10 \text{ MV m}^{-1}$) to affect the physical properties of the material. Therefore, understanding and controlling the flexoelectric effect is critical to the future of nanotechnology and electronics using nanoscale systems, such as thin-film heterostructures,^{4,5,14} extended structural defects such as domain walls,⁶ and nanocrystals.^{15–17}

Recent flexoelectricity studies have focused mostly on the ferroelectric properties of nanomaterials, because the generated electric field can be effectively coupled to the ferroelectric polarization. For example, the flexoelectric effect resulting from a nanoscale strain gradient has been shown to play an important role in novel ferroelectric functionalities, including domain control,⁴ mechanical switching of polarization,⁵ flexoelectric rotation of polarization,⁶ and the generation of new modulated phases at the morphotropic phase boundary.⁷

However, the ability of the nanoscale strain gradient to control other physical properties, such as electronic and magnetic properties,^{18,19} has received little consideration to date. The exploitation of such an effect would provide a general and viable way of designing the physical properties and associated functions of nanomaterials.

Here, we demonstrated the intriguing coupling between electronic transport and the mechanical strain gradient, emphasizing the potential key role of flexoelectricity in nanoelectronics. Epitaxial thin films can have a very large strain gradient (as large as 10^6 m^{-1}), because the misfit strain of a few percent can be relaxed within tens of nanometers (Figure 1a).⁴ The resulting internal flexoelectric field can have substantial effects in semiconductors with small band gaps, whose electrical transport depends strongly on the internal field.^{20,21} For our studies, we used 100-nm-thick epitaxial hexagonal HoMnO_3 (HMO) (0001) thin films grown on $\text{Pt}(111)/\text{Al}_2\text{O}_3(0001)$ substrates as a model system. HMO is known as a semiconducting dielectric material with a small band gap of $\sim 1.5 \text{ eV}$.²² Also, HMO has the lattice mismatch of +3.5% with the $\text{Pt}(111)/\text{Al}_2\text{O}_3(0001)$ substrate. Thus, this material offers a good opportunity to investigate how flexoelectricity can contribute to the electronic transport and functions.

Received: October 15, 2012

Revised: November 21, 2012

Published: November 28, 2012

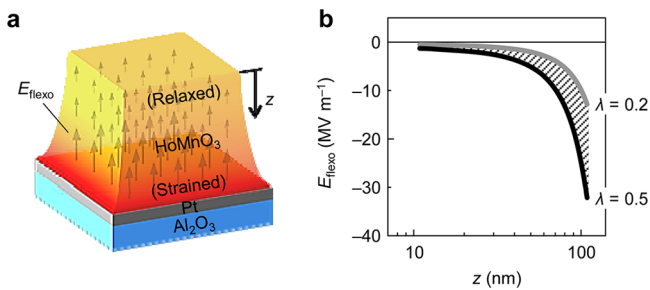


Figure 1. Nanoscale strain gradient in an epitaxial thin-film system. (a) Schematic diagram for (tensile) strain relaxation in epitaxial HoMnO₃ thin films, resulting in a nanoscale strain gradient. (b) Distribution of the estimated internal flexoelectric field (E_{flexo}) along the z direction, according to the chosen λ value (ranging from 0.2 to 0.5) in eq 1.

The internal electric field generated by flexoelectricity (E_{flexo}) may promote novel electronic phenomena. One possibility is unidirectional current flow, that is, the rectifying diode effect. We found that our epitaxial HMO thin films on Pt(111)/Al₂O₃(0001) substrates had a giant strain gradient of $\sim 10^6 \text{ m}^{-1}$.⁴ From the strain gradient measured by grazing incidence in-plane X-ray diffraction with synchrotron radiation, we roughly estimated the depth profile of the resulting E_{flexo} in our samples, using the following equation:^{11–13,23}

$$E_{\text{flexo}} = \lambda \frac{e}{\epsilon_0 a} \frac{\partial u}{\partial z} \quad (1)$$

where e is the electronic charge, ϵ_0 is the permittivity of free space, a is the lattice constant, u is the in-plane epitaxial strain, z

is the distance from the film surface, $\partial u / \partial z$ is the strain gradient, and λ is a constant close to unity. The exact λ value for HMO is not known, but λ in most oxide systems usually has a value on the order of unity.^{11–13} Figure 1b shows that, for a reasonable λ value between 0.2 and 0.5, the estimated internal field ($E_{\text{flexo}} \geq 10 \text{ MV m}^{-1}$) can be large and comparable to that in conventional p – n junctions or Schottky diodes.^{20,21,24} This implies that flexoelectricity produced by a nanoscale strain gradient can emerge as a practical means to tune electronic properties.

To explore the flexoelectric effect on electronic transport, we measured the local current–voltage (I – V) curves using conductive atomic force microscopy (C-AFM). Our results revealed several interesting features in the local transport of the epitaxial HMO film. First, in most regions of the film, the local I – V curves showed a rectifying behavior with a negative forward bias (i.e., the reverse diode effect), as shown in Figure 2a. The rectification ratio, defined as the ratio of the negative current divided by the positive current, was as large as 100 for $V = \pm 9 \text{ V}$. Second, there existed a strong inhomogeneity in the local transport. Along with a reverse diode effect in most regions, we observed a forward diode effect with a positive forward bias (Figure 2b) as well as a symmetric I – V curve (Figure 2c) in the other small regions. Figure 2d shows $2 \times 2 \mu\text{m}^2$ mapping images of the rectification ratios (i.e., $|I(-9 \text{ V})/I(+9 \text{ V})|$) for an epitaxial HMO film, highlighting both the dominant reverse diode effect and the strongly inhomogeneous local transport.

We first discuss why the reverse diode effect dominantly appeared in the epitaxial HMO films. The tensile strain gradient

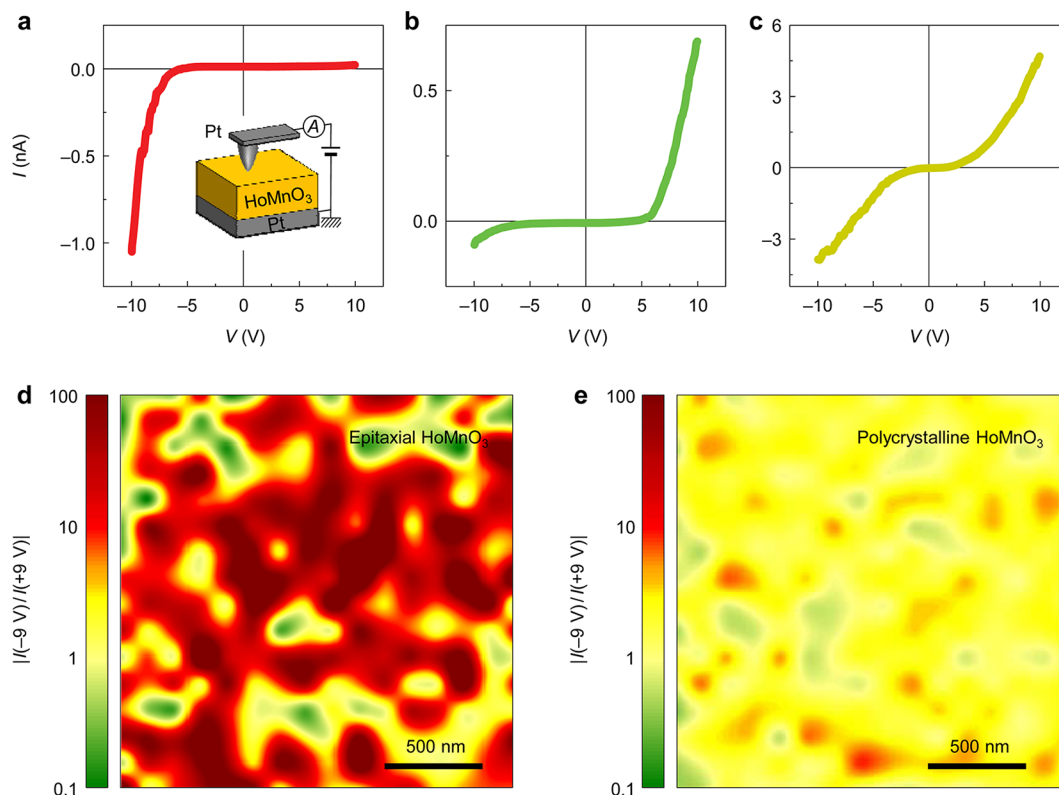


Figure 2. Flexoelectric effect on the local transport. (a–c) Local current–voltage (I – V) curves, measured by conductive atomic force microscopy (C-AFM) for epitaxial HoMnO₃ thin films. For the C-AFM measurements, we used a solid Pt nanowire tip. The reverse diode effect was dominant in the epitaxial HMO thin films, as shown in a. (d, e) Spatial distribution of local transport, measured for (d) epitaxial and (e) polycrystalline HoMnO₃ thin films. We mapped the measured rectification ratios (i.e., $|I(-9 \text{ V})/I(+9 \text{ V})|$) in the $2 \times 2 \mu\text{m}^2$ region with $\sim 100 \text{ nm}$ resolution.

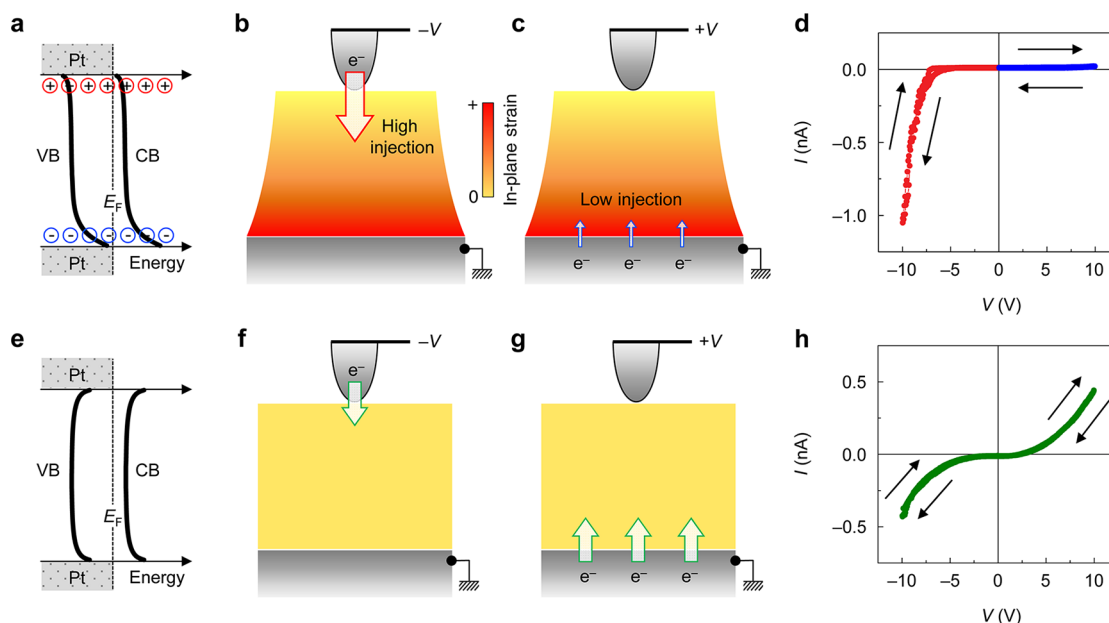


Figure 3. Flexoelectric rectifying diode effect. (a, e) Band characteristics for (a) epitaxial and (e) polycrystalline HoMnO₃ thin films. We assumed n-type conductivity of our films, since oxygen vacancies, the most common defects in oxides, can act as an electron donor. It should be noted that our concept should work well, not depending on the conductivity type. (b, c, f, g) Schematic diagrams of carrier injection according to the applied bias polarity for (b, c) epitaxial and (f, g) polycrystalline HoMnO₃ thin films. (d, h) Representative local $I-V$ curves for (d) epitaxial and (h) polycrystalline HoMnO₃ thin films.

and the associated E_{flexo} in the films can cause the upward flexoelectric polarization. Then, a positive (negative) bound charge is induced at the top (bottom) HMO/Pt interface, as schematically shown in Figure 3a. Independent measurements of surface charge density support the build-up of positive (negative) charge at the top (bottom) interface (Supporting Information, Figure S1). With this bound charge distribution,²⁴ the bottom interface may have a high Schottky barrier, while the barrier height at the top is small. A simple quantitative fit of the $I-V$ curve gives a Schottky barrier of ~ 0.5 eV, which is comparable to the value predicted from the flexoelectric effect (Supporting Information, Figures S2 and S3). With such an asymmetric Schottky barrier, the injection of electrons is more likely to occur at the top interface (Figures 3b and c). Thus, the large flexoelectric effect produced by the nanoscale strain gradient can induce unidirectional current flow, resulting in the observed reverse diode effect (Figure 3d).

We should note that the measured $I-V$ curves have nonhysteretic characteristics, as shown in Figure 3d. There are some other mechanisms for the rectifying conduction behavior, such as electromigration of charged ions²⁵ and the piezo/ferroelectric effect.²⁶ The $I-V$ curves for these other mechanisms usually involve a large hysteresis, whereas our $I-V$ results show little hysteresis. This suggests that our observed diode effect could originate from the mechanical strain gradient, which is robust under an external bias.

To obtain further insight, we measured the local $I-V$ curves for the 100-nm-thick polycrystalline HMO films grown on a Pt/Si(001) substrate, using C-AFM. The polycrystalline HMO films in Figure 2e exhibited symmetric $I-V$ behavior, with little diode effect (i.e., $|I(-9 \text{ V})/I(+9 \text{ V})| \approx 1$) in most regions. Due to the randomly oriented grains in the polycrystalline films, the average strain gradient field, especially normal to the film surface, is quite small (Supporting Information, Figure S4). With such a small strain gradient and symmetric electrode

geometry (as in our case), nearly symmetric Schottky barriers usually occur at each interface, due to the difference in the work functions of HMO and Pt (Figure 3e). This can induce nearly symmetric carrier injections (Figures 3f and g) and symmetric $I-V$ curves with weak back-to-back diode behavior (Figure 3h). Note that, for epitaxial and polycrystalline films, we used the same experimental conditions (i.e., the same electrode geometry and film deposition conditions), except for the substrates and the degree of the resulting strain gradient. Thus, the reverse diode effect in epitaxial HMO films should originate from the strain gradient, which was large enough to cause this phenomenon.

To verify the flexoelectric diode scenario more directly, we artificially generated a strain gradient in the polycrystalline HMO films. Lu et al. recently demonstrated that a high AFM tip force could generate a large strain gradient in the direction normal to the film surface,⁵ as schematically shown in Figures 4a and c. Following the same methodology, we measured the local $I-V$ curve for polycrystalline HMO films by varying the tip force. It was expected that an appreciable strain gradient would be generated with a high tip force, with a low tip force generating negligible strain gradient. We found that, with a high tip force, the local $I-V$ curves became asymmetric with a positive forward bias (Figures 4c and d), compared with the case using a relatively low tip force (Figures 4a and b). Thus, we can explain this result by the artificial generation of a strain gradient and associated E_{flexo} through the tip force, demonstrating the close correlation between the strain gradient and the observed diode effect.

Now we discuss the strong spatial inhomogeneity observed in the local transport of epitaxial HMO films (Figure 2d). Regions with an areal portion of $\sim 78\%$ exhibited the reverse diode effect, implying the dominant existence of upward E_{flexo} in the films. However, small regions with $\sim 10\%$ and $\sim 12\%$ areal portions exhibited the forward diode effect (Figure 2b)

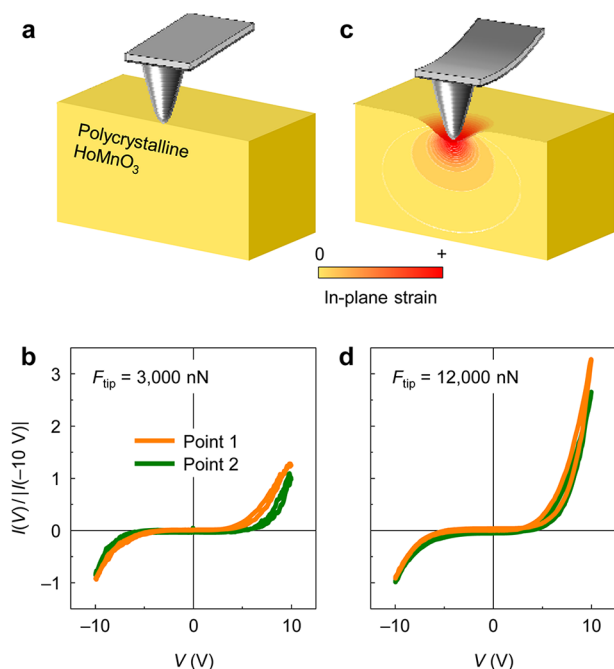


Figure 4. Artificial generation of the strain gradient. Local I - V curves of a polycrystalline HoMnO_3 thin film, measured using (a, b) normal loading and (c, d) high loading forces (F_{tip}) of an AFM tip.

and a symmetric I - V curve (Figure 2c), respectively. We observed that the polarity change of the diode effect occurred within a very short length scale (i.e., over a few hundred nanometers in epitaxial HMO films). This result implies the strong spatial inhomogeneity of the E_{flexo} direction and magnitude; some regions of 10% areal portion may exhibit a downward E_{flexo} , while other regions with 12% areal portion may have negligible E_{flexo} .

We can find a plausible explanation for the spatial inhomogeneity of E_{flexo} and the local transport by referring to the strain relaxation process. The relaxation of misfit strain in epitaxial films is usually accompanied by the formation of misfit dislocations,²⁷ one of the most common origins for strain relaxation. Near dislocations, there usually exists local inhomogeneities in the direction of the strain gradient; that is, the strain-gradient direction near dislocations can be opposite to that of the surrounding regions (Figure 5). Several previous theoretical and experimental studies have already shown the reverse strain-gradient direction near misfit dislocations in epitaxial thin-film systems.^{28,29} Thus, even if E_{flexo} in our films is mostly upward, it might be either downward or weak in small regions near the dislocations, resulting in strongly inhomogeneous local transport.

Our study emphasizes that flexoelectricity can provide important insight into nanotechnology and electronics. Specifically, we demonstrated that the flexoelectric effect at the nanoscale can generate a rectifying diode effect, which is essential for modern electronics.^{20,21} Also, it can govern the local transport characteristics, such as the spatial inhomogeneity of conduction, in thin-film epitaxy systems. As a material gets smaller in size, the strain gradient can become gigantic. Thus, the flexoelectric effect should be seriously considered in the design of electronic devices using nanoscale materials, such as nanowires and nanodots.^{15–17}

In conclusion, we demonstrated that the internal flexoelectric field induced by a nanoscale strain gradient can be large enough

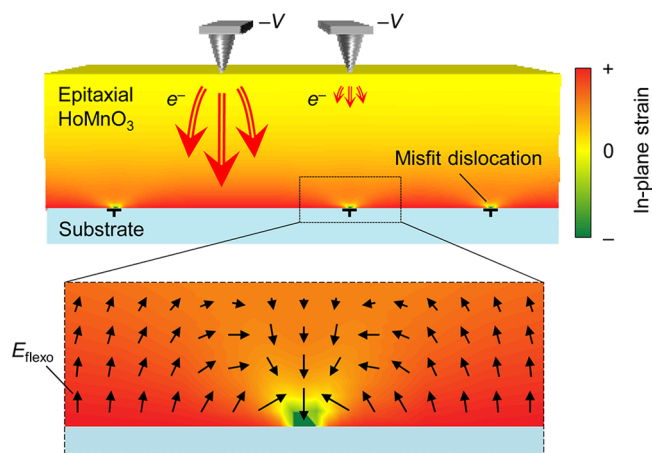


Figure 5. Possible origin of inhomogeneity in the strain-gradient direction. Near misfit dislocations, the direction of the strain gradient and the associated E_{flexo} can be reversed. As a result, strongly inhomogeneous local transport can occur.

to generate a rectifying diode effect. There are several noteworthy features of the flexoelectric diode effect. (1) Due to the universal nature of flexoelectricity, in principle, we can easily realize the diode effect in all dielectric materials. For example, perovskite-type dielectric materials with a small band gap, such as manganites and titanates, would provide further opportunity to study the flexoelectric diode effect more systematically (Supporting Information, Figure S5). (2) The flexoelectric diode effect originates from a purely mechanical strain gradient, completely different from conventional diodes that depend on the asymmetry of the system, such as p - n junctions or metal–semiconductor interfaces with Schottky barriers. (3) A flexoelectric diode does not require a complex junction structure like a p - n junction. Our results show that proper consideration of flexoelectricity would be required to advance novel nanoelectronic functionality.

■ ASSOCIATED CONTENT

Supporting Information

Methods and additional figures. This material is available free of charge via the Internet at <http://pubs.acs.org>.

■ AUTHOR INFORMATION

Corresponding Author

*E-mail: twnoh@snu.ac.kr.

Notes

The authors declare no competing financial interest.

■ ACKNOWLEDGMENTS

This work was supported by the Institute of Basic Science (IBS) (Grant No. EM1203) and the National Research Foundation of Korea (NRF) (Grant No. 2012-0005847; J.-G.Y.: No. 2011-0005145) grant funded by the Korea government (MEST). X-ray measurements were performed at the 10C1 beamline of Pohang Light Source. D.L. acknowledges support from the POSCO TJ Park Doctoral Foundation.

■ REFERENCES

- (1) Choi, K. J.; Biegalski, M.; Li, Y. L.; Sharan, A.; Schubert, J.; Uecker, R.; Reiche, P.; Chen, Y. B.; Pan, X. Q.; Gopalan, V.; Chen, L.-Q.; Schlom, D. G.; Eom, C. B. *Science* **2004**, 306, 1005–1009.

- (2) Zeches, R. J.; Rossell, M. D.; Zhang, J. X.; Hatt, A. J.; He, Q.; Yang, C.-H.; Kumar, A.; Wang, C. H.; Melville, A.; Adamo, C.; Sheng, G.; Chu, Y.-H.; Ihlefeld, J. F.; Erni, R.; Ederer, C.; Gopalan, V.; Chen, L. Q.; Schlom, D. G.; Spaldin, N. A.; Martin, L. W.; Ramesh, R. *Science* **2009**, *326*, 977–980.
- (3) Choi, W. S.; Kwon, J.-H.; Jeon, H.; Hamann-Borrero, J. E.; Radi, A.; Macke, S.; Sutarto, R.; He, F.; Sawatzky, G. A.; Hinkov, V.; Kim, M.; Lee, H. N. *Nano Lett.* **2012**, *12*, 4966–4970.
- (4) Lee, D.; Yoon, A.; Jang, S. Y.; Yoon, J.-G.; Chung, J.-S.; Kim, M.; Scott, J. F.; Noh, T. W. *Phys. Rev. Lett.* **2011**, *107*, 057602.
- (5) Lu, H.; Bark, C.-W.; Esque de los Ojos, D.; Alcalá, J.; Eom, C.-B.; Catalan, G.; Gruverman, A. *Science* **2012**, *336*, 59–61.
- (6) Catalan, G.; Lubk, A.; Vlooswijk, A. H. G.; Snoeck, E.; Magen, C.; Janssens, A.; Rispens, G.; Rijnders, G.; Blank, D. H. A.; Noheda, B. *Nat. Mater.* **2011**, *10*, 963–967.
- (7) Borisevich, A. Y.; Eliseev, E. A.; Morozovska, A. N.; Cheng, C.-J.; Lin, J.-Y.; Chu, Y. H.; Kan, D.; Takeuchi, I.; Nagarajan, V.; Kalinin, S. V. *Nat. Commun.* **2012**, *3*, 775.
- (8) Kogan, S. M. *Sov. Phys. Solid. State* **1964**, *5*, 2069–2070.
- (9) Tagantsev, A. K. *Phys. Rev. B* **1986**, *34*, 5883–5889.
- (10) Resta, R. *Phys. Rev. Lett.* **2010**, *105*, 127601.
- (11) Cross, L. E. *J. Mater. Sci.* **2006**, *41*, 53–63.
- (12) Zubko, P.; Catalan, G.; Buckley, A.; Welche, P. R. L.; Scott, J. F. *Phys. Rev. Lett.* **2007**, *99*, 167601.
- (13) Ma, W. *Phys. Status Solidi B* **2008**, *245*, 761–768.
- (14) Catalan, G.; Noheda, B.; McAneney, J.; Sinnamon, L. J.; Gregg, J. M. *Phys. Rev. B* **2005**, *72*, 020102.
- (15) Kalinin, S. V.; Meunier, V. *Phys. Rev. B* **2008**, *77*, 033403.
- (16) Landré, O.; Camacho, D.; Bougerol, C.; Niquet, Y. M.; Favre-Nicolin, V.; Renaud, G.; Renevier, H.; Daudin, B. *Phys. Rev. B* **2010**, *81*, 153306.
- (17) Bimberg, D.; Grundmann, M.; Ledentsov, N. N. *Quantum Dot Heterostructures*; John Wiley & Sons: Chichester, 1998.
- (18) Eliseev, E. A.; Morozovska, A. N.; Glinchuk, M. D.; Blinc, R. *Phys. Rev. B* **2009**, *79*, 165433.
- (19) Lukashev, P.; Sabirianov, R. F. *Phys. Rev. B* **2010**, *82*, 094417.
- (20) Kao, K.-C.; Hwang, W. *Electrical Transport in Solids with Particular Reference to Organic Semiconductors*; Pergamon Press: Oxford, 1981.
- (21) Sze, S. M.; Ng, K. K. *Physics of Semiconductor Devices*; Wiley Interscience: Hoboken, 2007.
- (22) Medvedeva, J. E.; Anisimov, V. I.; Korotin, M. A.; Mryasov, O. N.; Freeman, A. J. *J. Phys.: Condens. Matter* **2000**, *12*, 4947–4958.
- (23) Gruverman, A.; Rodriguez, B. J.; Kingon, A. I.; Nemanich, R. J.; Tagantsev, A. K.; Cross, J. S.; Tsukada, M. *Appl. Phys. Lett.* **2003**, *83*, 728–730.
- (24) Pintilie, L.; Alexe, M. *J. Appl. Phys.* **2005**, *98*, 123103.
- (25) Waser, R.; Aono, M. *Nat. Mater.* **2007**, *6*, 833–840.
- (26) Blom, P. W. M.; Wolf, R. M.; Cillessen, J. F. M.; Krijn, M. P. C. *M. Phys. Rev. Lett.* **1994**, *73*, 2107–2110.
- (27) Hirth, J. P.; Lothe, J. *Theory of Dislocations*; Wiley: New York, 1982.
- (28) Chu, M. W.; Szafraniak, I.; Scholz, R.; Harnagea, C.; Hesse, D.; Alexe, M.; Gosele, U. *Nat. Mater.* **2004**, *3*, 87–90.
- (29) Nagarajan, V.; Jia, C. L.; Kohlstedt, H.; Waser, R.; Misirlioglu, I. B.; Alpay, S. P.; Ramesh, R. *Appl. Phys. Lett.* **2005**, *86*, 192910.